## ORIGINAL RESEARCH

# A novel prognostic index based on autophagy-related genes—the Achilles' heel of cervical squamous cell carcinoma

Li Zhu[1],*, Yaqiong Guo[1], Huijuan Yan[1], Yuan Wen[1]

[1]Department of Obstetrics and
Gynecology, Yellow River Sanmenxia
Affiliated Hospital of Henan University of
Science and Technology, 472000
Sanmenxia, Henan, China

*Correspondence
dorlizhulab@126.com
(Li Zhu)

### Abstract

Despite sustained advances in the diagnosis and treatment of cervical squamous cell carcinoma (CESC), patients with advanced or recurrent CESC are prone to a poor prognosis. Accumulating evidence suggests that autophagy-related genes (ARGs) are prominent indicators of CESC prognosis. Transcriptomic and clinical data of CESC patients were obtained from The Cancer Genome Atlas (TCGA) database to calculate an autophagy-related gene prognostic index (API) based on the hub genes using a least absolute shrinkage and selection operator (Lasso)-Cox regression model. Its efficacy in predicting the overall survival (OS) and immunotherapeutic responses of CESC patients was assessed. Three autophagy-related genes, *B cell leukemia/lymphoma 2* (*BCL2*) and *tumor protein p73* (*TP73*), were independent prognostic factors of CESC and were used to obtain API. Patients with high API showed better OS, along with enhanced infiltration of (cluster of differentiation 8$^+$) CD8$^+$ T and Treg cells, inhibition of activated natural killer (NK) cells, and activation of dendritic cell infiltration in CESC tissues. As compared to those with low API, patients with a high API showed enhanced expressions of immune checkpoints, including *programmed death-1* (*PD-1*), *programmed death-ligand 1* (*PD-L1*), and *cytotoxic T-lymphocyte associated protein 4* (*CTLA4*), and lower half maximal inhibitory concentration (IC$_{50}$) values for common chemotherapy agents, including paclitaxel and cisplatin. Collectively, low expression of ARGs, namely *BCL2* and *TP73*, may be the Achilles' heel for CESC. API could accurately predict the prognosis and efficacy of immunotherapy and chemotherapy for CESC patients.

### Keywords

Cervical squamous cell carcinoma; Prognosis; Immunotherapy; Chemotherapy

## 1. Introduction

Cervical squamous cell carcinoma (CESC) is the second most common tumor in women, with approximately 500,000 new cases and 300,000 deaths annually, worldwide. It is the leading cause of cancer-related death among women [1]. Patients with early-stage (stage I/II) CESC often show a favorable prognosis; however, for those with advanced (stage III/IV) or metastatic CESC, the prognoses are inevitably disappointing owing to limited treatment options, which remain confined to a combination of radiotherapy, immunotherapy, chemotherapy, and targeted therapy [2, 3]. The 5-year progression-free survival (PFS) and overall survival (OS) of these patients are 51% and 55%, respectively [4]. Accumulating evidence suggests that immunotherapy is a promising treatment strategy, and may improve the prognosis of patients with advanced or recurrent CESCs.

Treatment with immune checkpoint inhibitors (ICIs), such as *programmed death-ligand 1* (*PD-L1*), *programmed death*

*receptor 1* (*PD-1*), and *cytotoxic T lymphocyte-associated antigen-4* (*CTLA4*) inhibitors, is effective in improving prognosis in various cancer types as compared to conventional treatment [5, 6]. It offers hope for patients with advanced metastatic or recurrent CESC and can be included in palliative treatment [7, 8]. However, the caveat to ICI treatment is the response of individual patients, some of whom may benefit insufficiently from ICIs or show an inadequate response thereto, thus limiting the wider application of ICIs [9]. Analysis of the immune cell infiltration landscape, reflective of the patient's response to ICIs, may yield new biomarkers for prognostic prediction of CESC [10]. However, more biomarkers are required to evaluate ICI's ICI treatment efficacy.

Autophagy is the process of degradation and recycling of proteins and intracellular components during starvation or stress [11]. It is strongly associated with tumor cell behavior, inhibiting tumor occurrence and progression in the early stages of tumorigenesis, while stimulating tumor growth and

invasiveness in the later stages [12]. More importantly, by receiving various stimuli from the tumor microenvironment (TME), autophagy pathways in tumor and immune cells can be altered, resulting in differential effects on tumor progression, immune response, and therapy [13]. In tumor cells, autophagy pathways are closely related to inflammation and cell death pathways, thereby altering the immunogenicity of TME and anti-tumor immune responses [14]. Therefore, autophagic components are valuable targets for enhancing immune abundance in TME and immune cell functions in immunotherapy; autophagy-related molecules may serve as inducible markers of tumor occurrence and progression [15].

This study aimed to identify prognostic markers for CESC to predict the prognosis following conventional therapy versus immunotherapy. Based on the autophagic components in tumors, hub autophagy-related genes (ARGs) associated with patient prognosis were screened. We aimed to construct an autophagy-related prognostic index (API) to predict prognosis and ICI efficacy in CESC patients. Subsequently, the molecular and immune characteristics of APIs were characterized, and its prognostic prediction ability for patients who underwent immunotherapy was determined. The immunogenetic profiles were also characterized.

# 2. Materials and methods

## 2.1 Data acquisition

Transcriptome, clinical, and somatic mutation data of 309 samples, including three normal cervical tissues and 306 CESC tumor tissues, were extracted from The Cancer Genome Atlas (TCGA) (https://portal.gdc.cancer.gov/). A gene list comprising 231 ARGs was obtained from the Human Autophagy Database (http://www.autophagy.lu/index.html).

## 2.2 API generation and validation

The transcriptome was analyzed to identify differentially expressed genes (DEGs) between normal and tumor tissues. Genes fulfilling the cut-off criteria of fold-change (FC) absolute value $>1$ and false discovery rate (FDR) $<0.05$ were selected. Among these, autophagy-related differentially expressed genes (AEGs) were further analyzed. Their biological functions were assessed by Gene Ontology (GO) and Kyoto Encyclopedia of Genes and Genomes (KEGG) enrichment analyses using the clusterProfiler package in R (version 4.0.2, 2020). An adjusted $p$-value of $< 0.05$ was set as the cutoff to filter significant functions.

Gene expression profiles and patient survival data were integrated followed by the random division of tissue samples into a training set (n = 184) and a testing set (n = 90). The clinical features of the two sets were compared to examine intergroup homogeneity. Univariate Cox regression analysis was performed to identify prognostic AEGs in CESC tumor tissues in the training set. The best prognostic prediction model was constructed by LASSO Cox regression, wherein the API represented the efficacy index. The efficacy of API in predicting the OS of patients with CESC was validated in the testing set. All patients were assigned to either high

or low API groups based on the median API value obtained in the training set. Patient OS between the two groups was compared by Kaplan-Meier (KM) survival analysis. Receiver operating characteristic (ROC) curves were plotted to evaluate the predictive accuracy of API. Based on survival status and AEGs, risk curves were plotted to identify high-risk ARGs in CESC. The independence of API for prognostic prediction was evaluated by univariate and multivariate Cox regression analyses.

## 2.3 Profiling of immune cells and immune checkpoint genes

Differences in 22 infiltrating immune cell types between CESC and normal cervical tissues, and patients with high versus low API were compared by cell type identification by estimating relative subsets of RNA transcripts (CIBERSORT) algorithm [16], and potential correlations between API and infiltrating immune cells in CESC were assessed to determine the prognostic value of the former. Differences in the expression of immune checkpoint genes (*PD-1*, *PD-L1*, *PD-L2*, *CTLA4*, *lymphocyte activating 3* (*LAG3*), *hepatitis A virus cellular receptor 2* (*HAVCR2/TIM3*), *T cell immunoreceptor with Ig and ITIM domains* (*TIGIT*), and *V-set immunoregulatory receptor* (*VISTA*)), and somatic mutations in tumorous tissues were compared between the patients with high and low API. The landscape of mutation profiles between high and low API groups was visualized using waterfall plots drawn using maftools in R.

## 2.4 Predicting efficacy of ICIs and targeted therapies using API

The sensitivity of API in predicting the efficacy of common ICIs was assessed using relevant data from the Cancer Immunome Atlas (TCIA) database (https://tcia.at/home) with a comprehensive view of the immunogenomic landscape of 20 solid cancers. The "pRRophetic" package in R was utilized for chemosensitivity analysis. The efficacy of common ICIs and two first-line chemotherapy agents (paclitaxel and cisplatin) was compared between patients with high versus low API. Sensitivity to chemotherapy was determined by the half-maximal inhibitory concentration ($IC_{50}$).

## 2.5 Establishment of a nomogram for survival prediction

We performed a joint regression analysis for the expression profiles of hub ARGs and clinicopathological data using the "rms" package in R and obtained a clinicopathologic genomic nomogram. Calibration curves were drawn for predicting OS in CESC. The points (rating score) for each component in the nomogram were calculated, and the OS rates of patients with CESC were estimated according to the sum score. Correction curves for the discrete degrees of actual versus predicted values were plotted to assess the prediction accuracy of the nomogram.

## 2.6 Statistical analysis

All statistical analyses were performed using R (version 4.0.2, 2020) and SPSS (version 26, SPSS Inc., Chicago, IL, USA). Log-rank and Wilcoxon tests were separately utilized for comparisons of survival data and continuous variables. The *chi-squared* test was used to compare the distribution of discontinuous variables. Correlation analyses were performed using the Spearman test. A two-tailed $p$-value $< 0.05$ denoted statistical significance.

## 3. Results

### 3.1 Expression and biofunctions of 35 AEGs in CESC

Transcriptome analysis yielded 3428 DEGs in CESC tissues, wherein 1845 were upregulated while 1583 were downregulated. Their distributions were visualized using volcano maps (Fig. 1A). This set of DEGs was intersected with 231 ARGs to obtain AEGs in CESC tissues, and 35 genes whose expression patterns were significantly different from those in normal tissues were identified (**Supplementary Table 1**), as shown in the Venn diagram (Fig. 1B,C). GO analysis showed that these AEGs were mainly enriched in biological processes (BP) involved in apoptotic signaling; cellular components (CC) including the mitochondrial outer membrane, organelle outer membrane, and nuclear envelope, and molecular functions (MF) of ubiquitin protein ligase binding, ubiquitin-like protein ligase binding, and transcription factor-DNA binding (Fig. 1D). KEGG analysis suggested that apoptosis and p53 signaling were significantly associated with these AEGs (Fig. 1E).

### 3.2 Establishment and validation of API

The above-mentioned 35 AEGs were subjected to univariate Cox regression, and three hub genes (*BCL2*, *autophagy related 4D cysteine peptidase* (*ATG4D*), and *TP73*) were found to be significantly correlated with the survival of patients with CESC, as shown in the forest map (Fig. 2A). Among them, *BCL2* and *TP73* were included in the Lasso-Cox regression model for obtaining the API (Fig. 2B,C). The API score was calculated as follows: API = $(0.3602 \times \text{Exp}_{BCL2}) + (0.2656 \times \text{Exp}_{TP73})$, wherein, Exp indicates the gene expression and the numbers represent weight scores, indicating the impact of the corresponding gene expression on the prognosis of patients; the higher the value, the greater the impact on the prognosis. The KM survival curves for the training set ($p = 0.016$), testing set ($p = 0.045$), and all patients ($p = 0.004$) showed that those with a low API had significantly shorter OS than those with high API (Fig. 2D), with area under the curves (AUCs) of 0.655, 0.785, and 0.706, respectively (Fig. 2E). This suggested satisfactory prediction accuracy of the API for patient survival. Univariate and multivariate Cox regression analyses demonstrated that stage classification ($p = 0.002$) and API ($p < 0.001$) were independent prognostic factors for CESC (Fig. 3A,B). The risk curves for the distribution of death revealed a lower number of deaths and reduced death risk in patients with high API as compared to those with low API

(Fig. 3C–E). Characteristic of the calculated APIs in high and low riks group of CESE is shown in **Supplementary Table 2**.

Gene expression data of hub AEGs, along with age and staging, were used to construct a prognostic nomogram for estimating the survival probability of patients with CESC. The predicted 1-, 2- and 3-year OS rates, calculated according to the sum of each component score of the nomogram, were very close to the actual values (Fig. 3F,G). This suggested an accurate prediction ability of the clinicopathologic genomic nomogram.

### 3.3 Immunological characteristics of CESC tissues in patients with high versus low API

CIBERSORT was utilized for immune cell profiling in CESC versus normal cervical tissues and patients with high versus low API. Cell expression signatures were extracted from CESC RNA sequencing (RNA-seq) data after excluding those with inaccurate sample results ($p$-value $\geq 0.05$), comprising a total of 60 CESC samples. The results showed significantly enhanced infiltration of resting memory CD4$^+$ T cells and M1/M2 macrophages in CESC versus normal cervical tissues (Fig. 4A,B). KM survival analysis suggested that patients with increased infiltration of activated memory CD4$^+$ T cells ($p < 0.001$) and CD8$^+$ T cells ($p = 0.049$) showed longer OS (Fig. 4C). Compared to those with a high API, reduced infiltration of naïve B cells ($p = 0.008$), resting memory CD4$^+$ T cells ($p = 0.041$), activated memory CD4$^+$ T cells ($p = 0.005$), and resting dendritic cells (DCs) ($p = 0.012$) but elevated abundances of activated NK cells ($p = 0.005$), M0 macrophages ($p = 0.007$), and eosinophils ($p = 0.002$) were observed in patients with low API (Fig. 4D). High API scores were associated with enhanced infiltration of CD8$^+$ T cells ($R = 0.19$, $p = 0.014$), regulatory T cells (Tregs) ($R = 0.23$, $p = 0.004$), resting memory CD4$^+$ T cells ($R = 0.16$, $p = 0.038$), monocytes ($R = 0.21$, $p = 0.009$), and naïve B cells ($R = 0.28$, $p < 0.001$), and attenuated infiltration of activated mast cells ($R = -0.26$, $p < 0.001$), neutrophils ($R = -0.18$, $p = 0.027$), activated NK cells ($R = 0.001$) $= -0.16$, $p = 0.045$), activated DCs ($R = -0.19$, $p = 0.018$), eosinophils ($R = -0.28$, $p < 0.001$), and M0 macrophages ($R = -0.22$, $p = 0.005$) (Fig. 4E).

Subsequently, somatic mutation analysis was performed to determine whether mutation frequency and tumor mutation load could account for the differences in immune infiltration between the two API groups. As shown in the waterfall plot (Fig. 5A,B), somatic mutations were frequently observed in CESC tissues, and nearly 88.5% of them occurred in patients with a high API. Mutations in *Titin* (*TTN*), *phosphatidylinositol-4,5-bisphosphate 3-kinase catalytic subunit alpha* (*PIK3CA*), *lysine methyltransferase 2C* (*KMT2C*), *mucin 4, cell surface associated* (*MUC4*), and *MUC16* were frequently observed, most of which were of the missense type.

Differences in the expression of the eight most common immune checkpoint genes between patients with high and low API were examined. Among these, six, including *PD-1* ($p = 0.024$), *PD-L1* ($p = 0.009$), *CTLA4* ($p = 0.014$), *TIM-3* ($p = 0.042$), *TIGIT* ($p < 0.001$), and *VISTA* ($p = 0.046$) were elevated in patients with high API. No significant differences were observed in the levels of *PD-L2* ($p = 0.32$) and *LAG3* ($p$
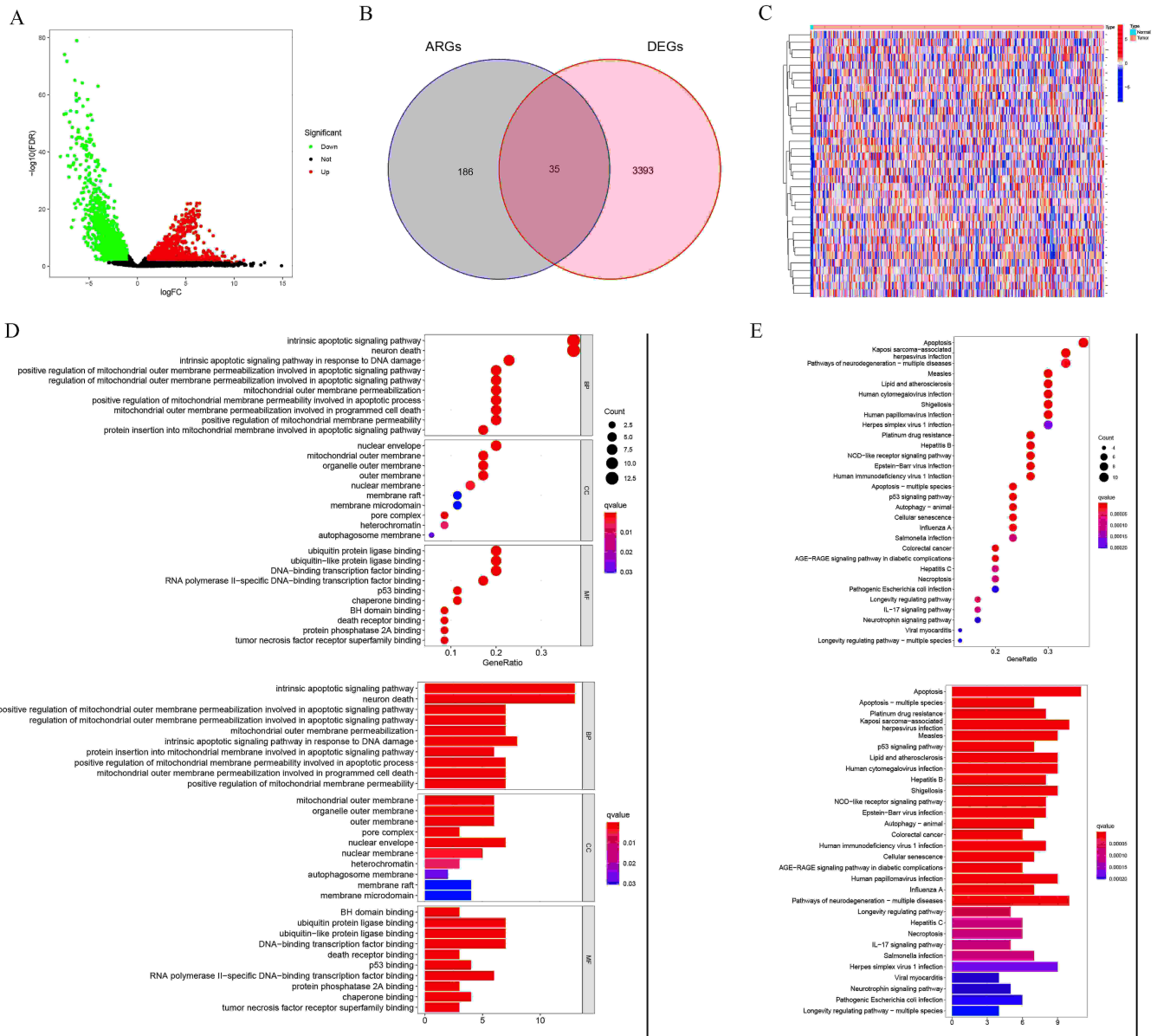
**FIGURE 1. Identification of autophagy-related differentially expressed genes (AEGs) in CESC.** (A) Volcanic maps show the gene expression profile in CESC versus normal tissues. (B) Intersection of differentially expressed genes (DEGs) with autophagy-related genes (ARGs). (C) The thermogram reveals the pattern of expression of 35 AEGs in CESC. Blue and red indicate down-regulated and up-regulated ARGs, respectively. (D) GO enrichment analysis. (E) KEGG enrichment analysis. The abscissa of the bubble diagram indicates the proportion of genes in each KEGG pathway. The bubble size indicates the number of enriched genes. Blue and red represent low and high significance, respectively. The abscissa of the histogram represents the number of genes assigned to each enrichment result. Blue and red represent low and high significance, respectively. CESC: cervical squamous cell carcinoma; GO: gene ontology; KEGG: kyoto encyclopedia of genes and genomes.

= 0.07) between the two groups (Fig. 5C).

## 3.4 API predicts the efficacy of immunotherapy and chemotherapy in CESC patients

Compared to patients with low API, those with high API showed greater benefits from *CTLA4* and *PD-1* inhibitors ($p$ = 0.042) (Fig. 6A) and higher sensitivity (lower $IC_{50}$ values) to paclitaxel ($p$ = 0.0092) and cisplatin ($p$ = 0.00046) (Fig. 6B). Therefore, patients with high API may show adequate responses to common ICIs or chemotherapeutic agents. The risk model allowed for the prediction of prognosis, and efficacy of immunotherapy and chemotherapy for CESC patients, which is expected to provide a reference for future clinical trials.

## 4. Discussion

ICIs are effective for relapsed or refractory CESC [17, 18] but their application remains unsatisfactory owing to fluctuating overall response rates (ORRs). Several recent studies on ICIs describe promising preliminary results using a combination of ICIs, radiotherapy, and chemotherapy in patients with cancer
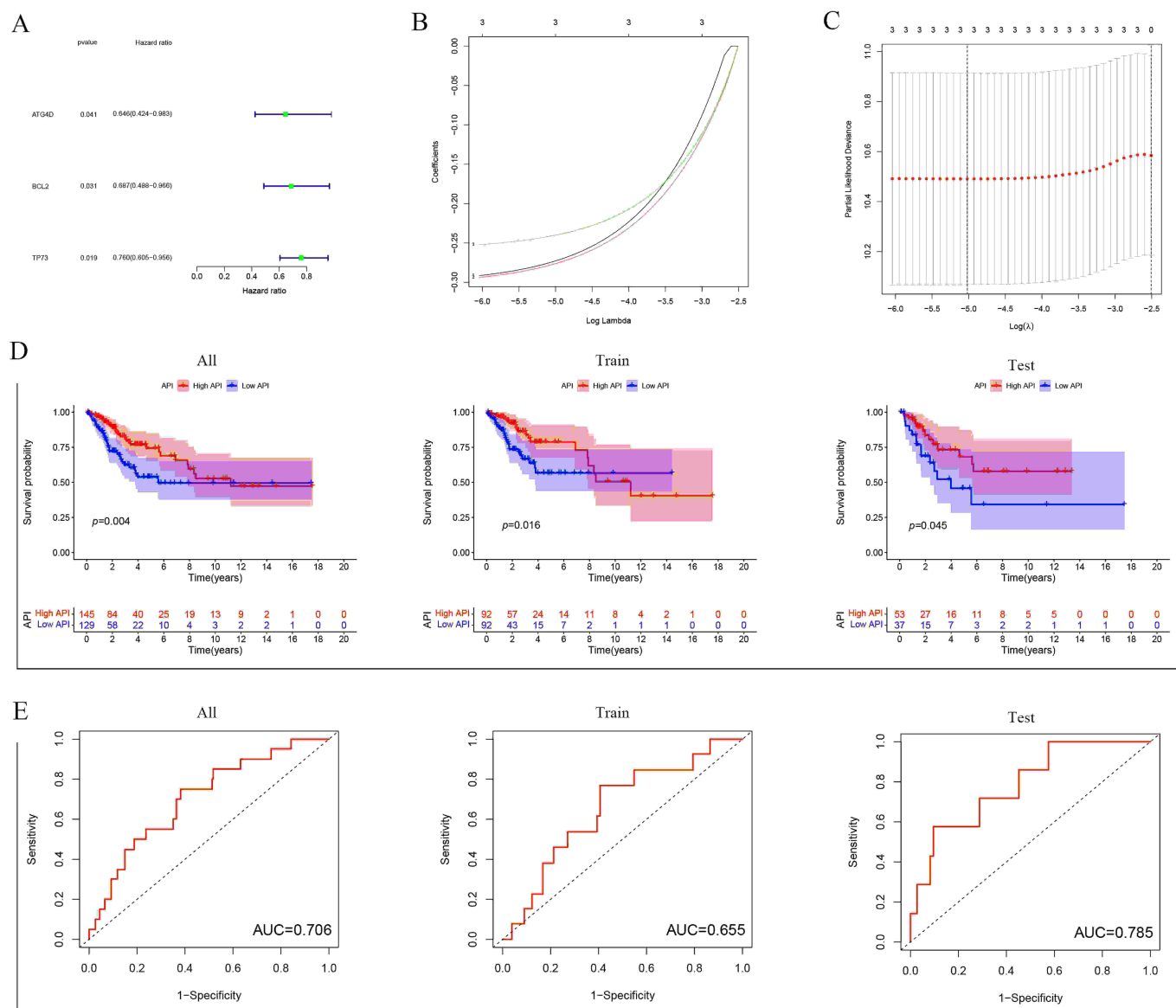
**FIGURE 2. Establishment and validation of the API.** (A) Three prognostic AEGs were used for API generation. (B) A Lasso model was adopted to predict the trajectory of each independent variable. The horizontal axis represents the logarithmic value of the independent variable λ, and the vertical axis represents the coefficient of the independent variable. (C) Confidence interval for each λ in the Lasso model. (D) KM survival curves for overall survival prediction for patients with high versus low API. (E) ROC curves reveal the satisfactory predictive ability of API. ATG4D: autophagy related 4D cysteine peptidase; BCL: B cell leukemia/lymphoma 2; TP73: tumor protein p73; API: autophagy-related gene prognostic index; AUC: area under the curves.

to achieve a high ORR [19, 20]. The expression of traditional biomarkers such as *PD-1/PD-L1* or *CTLA4* is unable to accurately predict ICI sensitivity [10]. Therefore, effective biomarkers to predict prognosis and potential immunotherapeutic benefits are lacking, thus highlighting the importance of identifying such biomarkers for CESC.

Autophagy is a catabolic process in response to cellular stress, which can promote tumorigenesis, tumor growth, and tumor progression, and suppress tumor initiation [21]. It also controls the homeostasis of immune cells in the TME, thus determining the survival, activation, proliferation, and differentiation of NK cells, macrophages, DCs, and T and B lymphocytes [22]. Amongst several autophagic stimuli, immunosuppressive *PD-L1/PD1* engagement triggers T-cell autophagy, thus helping tumor cells evade immune surveil-

lance and generate intrinsic drug resistance to immunotherapy [23, 24]. The relationship between autophagy and other immunotherapeutic agents and immune-mediated mechanisms of antitumor activity has been reported previously [25]. In general, autophagy has a complex relationship with the antitumor immune system, which can participate in regulating immune responses in the TME in several ways. Autophagy-related biomarkers can be used for the evaluation and monitoring of immunotherapeutic efficacy and prognostic prediction in cancer patients [26].

ARGs are a set of genes involved in autophagy [27]. In the current study, we identified 35 AEGs in CESC tissues; among them, two, namely *BCL2* and *TP73*, were the most significantly related genes with the risk of CESC progression. These were included for obtaining the API using a Lasso-Cox
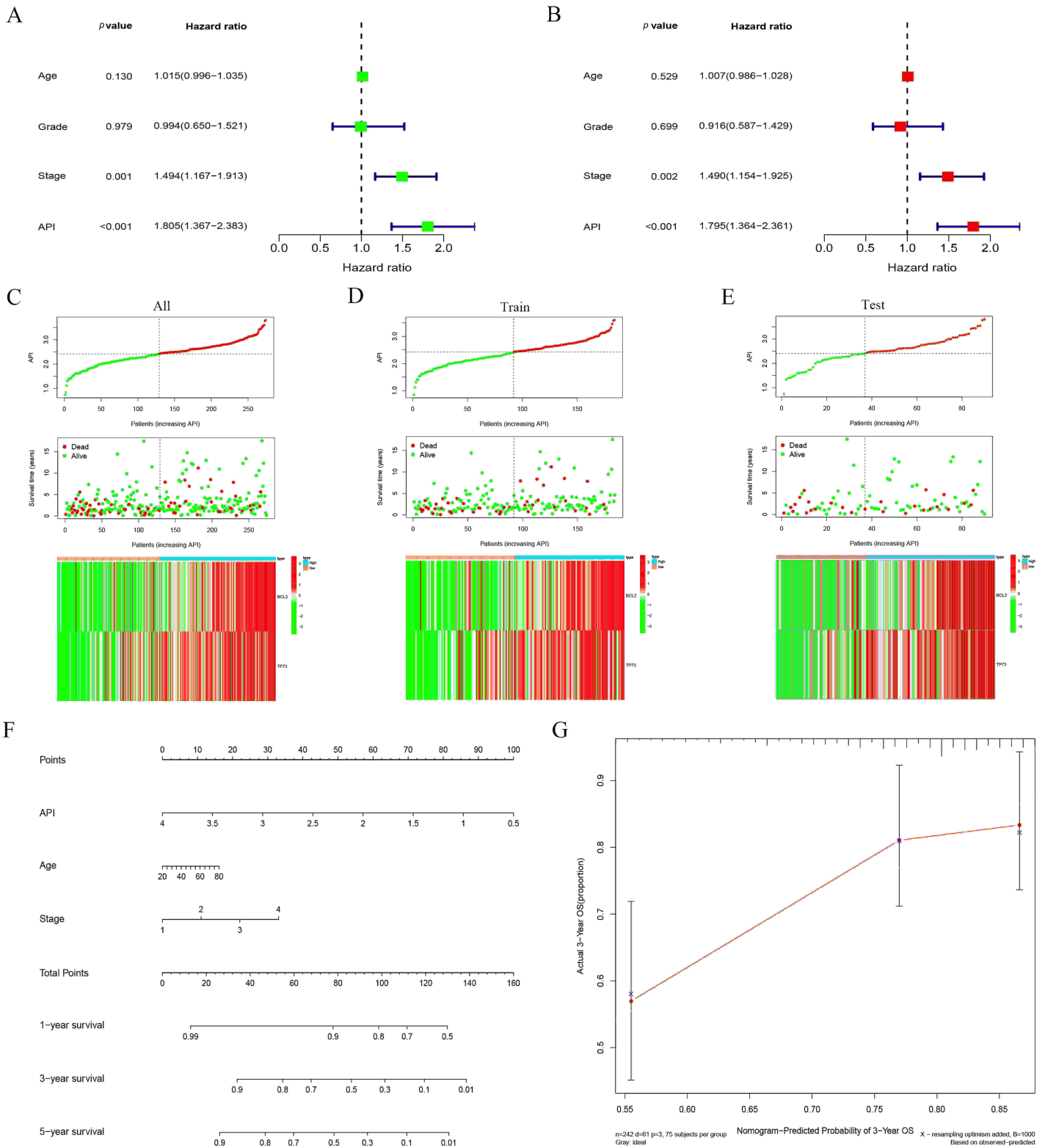
**FIGURE 3. Independence of API in the prognostic prediction of CESC and construction of a nomogram.** (A,B) Univariate and multivariate Cox regression analyses indicate API as an independent prognostic indicator. (C–E) Distribution of API score, OS, and hub gene expression in patients from the training and testing sets and all patients. (F,G) Calibration curves show the accuracy of the nomogram for predicting 1-, 3- and 5-year OS rates for CESC patients. API: autophagy-related prognostic index; OS: overall survival.
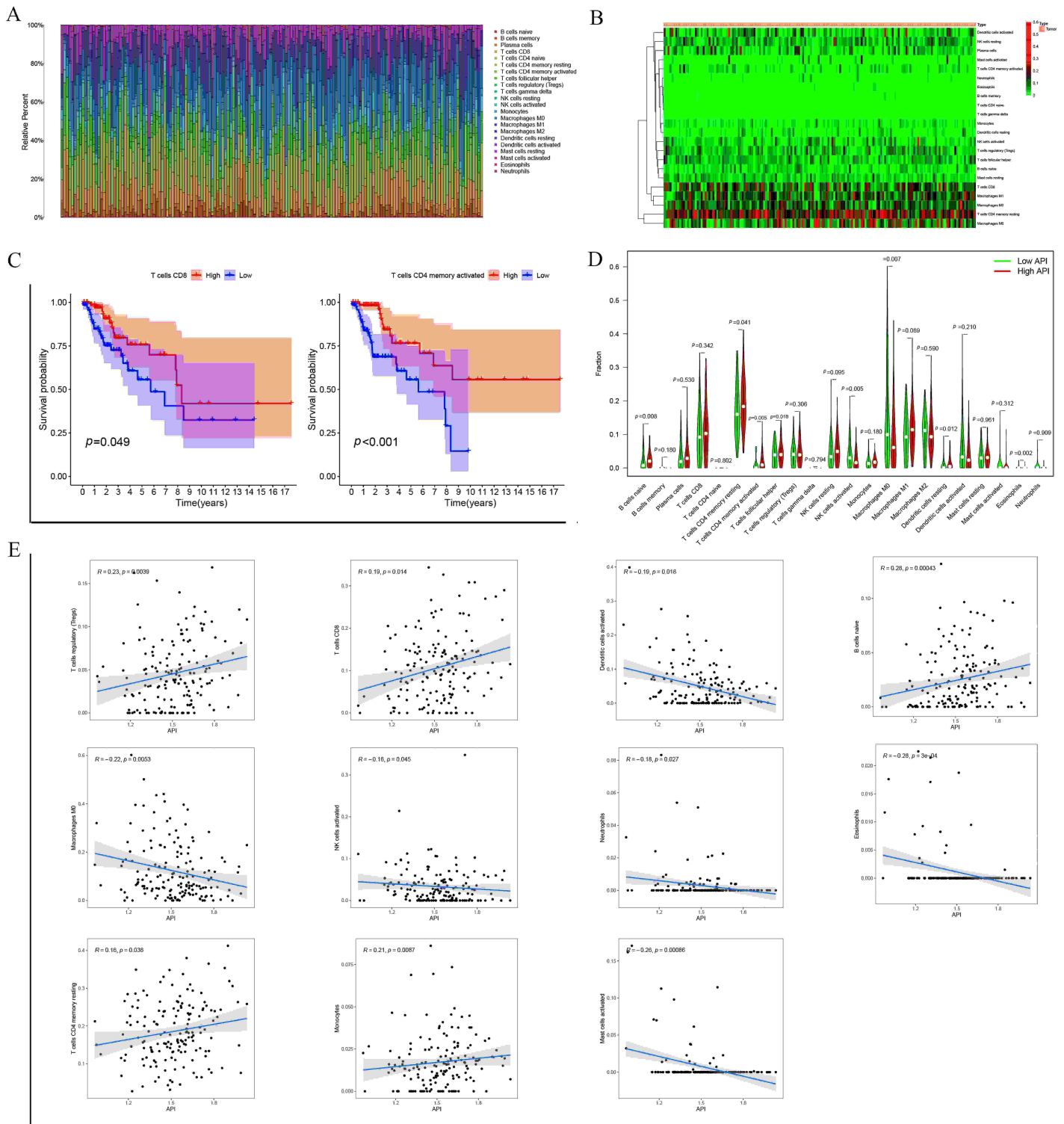
**F I G U R E 4. Profiling of tumor-infiltrating immune cells in CESC.** (A) Profiling of 22 types of immune cells in CESC. (B) The thermogram shows the degree of infiltration of 22 immune cells in CESC tissues. (C) The KM survival analysis characterizes the immune cell landscape for patients with longer OS. (D) Differences in the immune cell landscape between patients with high and low API. (E) Correlation of the API score with tumor-infiltrating immune cells in CESC. CESC: cervical squamous cell carcinoma; KM: Kaplan-Meier; OS: overall survival; API: autophagy-related prognostic index.
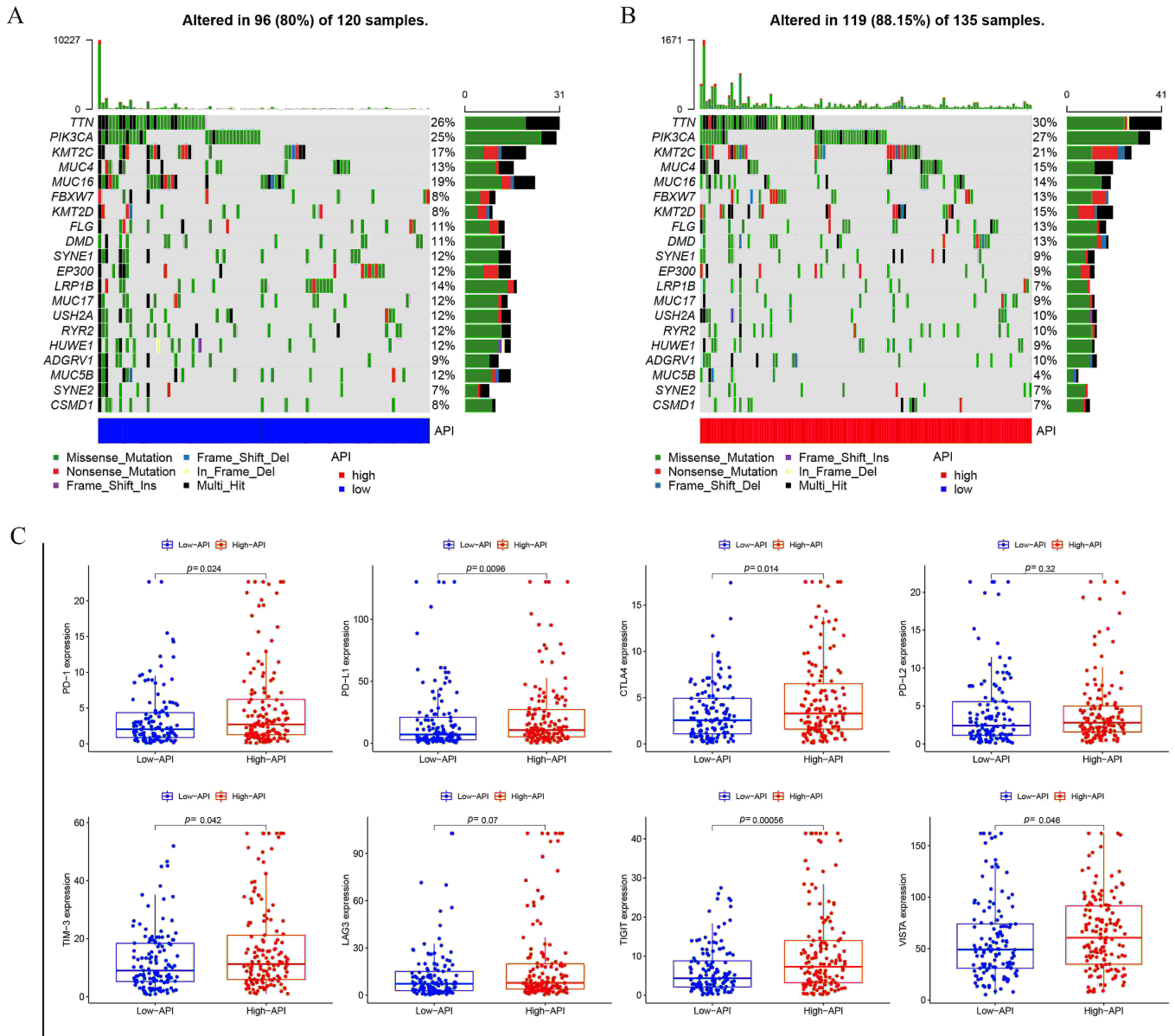
**FIGURE 5. Gene mutation landscape and immune checkpoint gene expression in patients with high versus low API.** (A,B) The waterfall plot shows somatic mutations in patients with high versus low API. (C) Expression of the six immune checkpoint genes is elevated in patients with high versus low API. API: autophagy-related prognostic index. TTN: titin; KMT2C: lysine methyltransferase 2C; MUC4: mucin 4, cell surface associated; MUC16: mucin 16, cell surface associated; FBXW7: F-box and WD repeat domain containing 7; KMT2D: lysine methyltransferase 2D; FLG: filaggrin; DMD: dystrophin; SYNE1: spectrin repeat containing nuclear envelope protein 1; EP300: E1A binding protein p300; LRP1B: LDL receptor related protein 1B; MUC17: mucin 17, cell surface associated; USH2A: usherin; RYR2: ryanodine receptor 2; HUWE1: HECT, UBA and WWE domain containing E3 ubiquitin protein ligase 1; ADGRV1: adhesion G protein-coupled receptor V1; MUC5B: mucin 5B, oligomeric mucus/gel-forming; SYNE2: spectrin repeat containing nuclear envelope protein 2; CSMD1: CUB and Sushi multiple domains 1.

model. Anti-apoptotic *BCL2* family of proteins is important in promoting cell growth and maintaining cell survival [28]. The *BCL2* gene encoding *BCL2* is strongly associated with better prognosis in various tumor types [29, 30]. *TP73*, a member of the *TP53* family, is also involved in tumor occurrence and progression [31]. It is downregulated in tumor tissues in the early clinical stages and is negatively associated with lymph node or distant metastasis. Patients with CESC showing high *TP73* expression often have low-grade tumors and longer

OS, and thus, *TP73* is a promising biomarker for prognostic prediction in CESC [32]. In this study, patients with high API showed prolonged OS as compared to those with low API. Although the survival curves intersected at 50% survival, it does not imply that patients with low API have better OS in the later stages. Before the intersection (11th year), only 3 patients had low API, while 10 had high API. A patient with high API died, resulting in the intersection of curves at the corresponding time; thus, a 50% survival rate did not
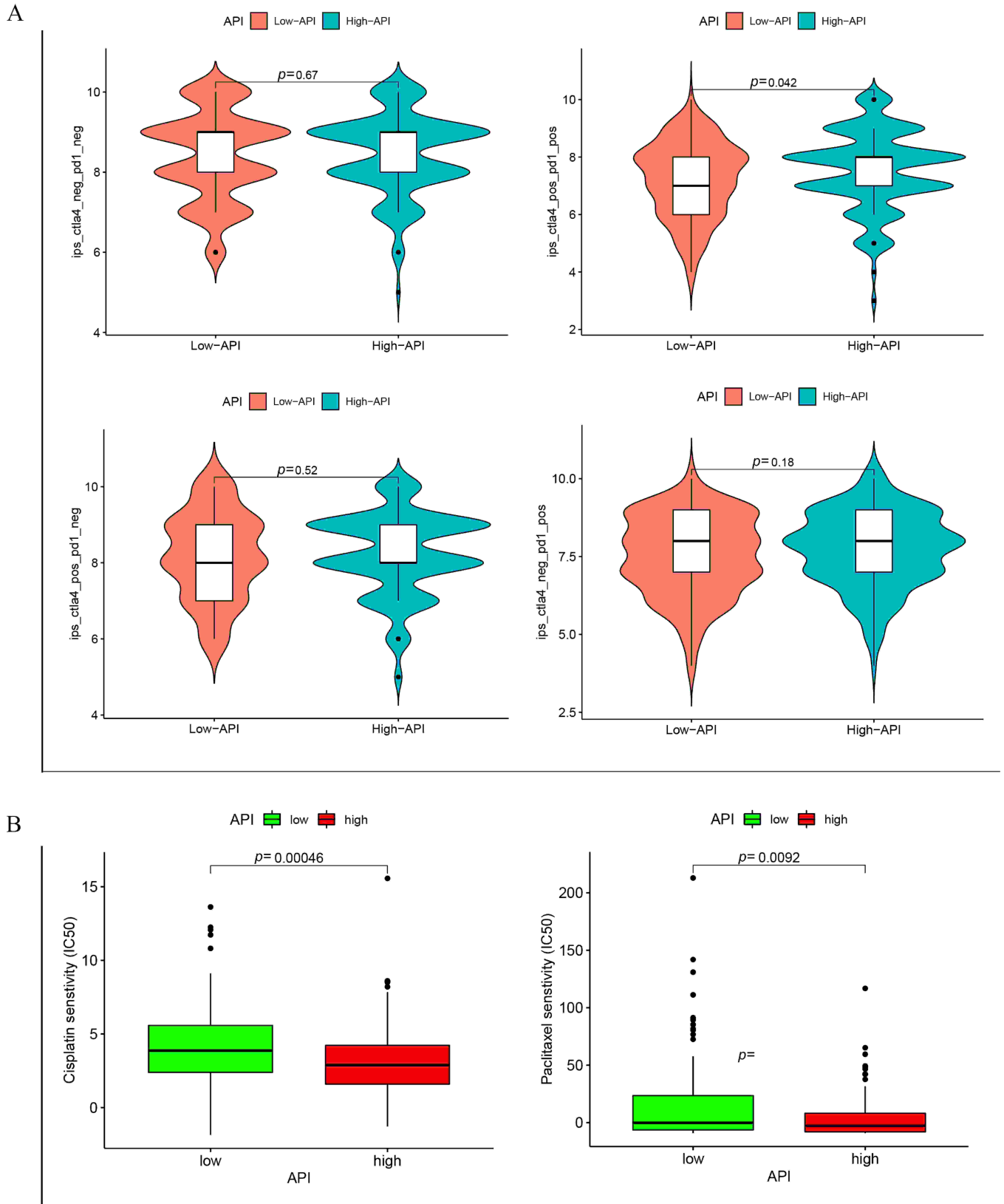
A



B



**FIGURE 6. API predicts the efficacy of immunotherapy and chemotherapy in CESC patients.** (A) The analysis of immunotherapeutic efficacy based on API reveals an inadequate response to anti-*CTLA4* and anti-*PD1* drugs in high-risk CESC patients. However, there were no differences in the responses of patients on anti-*CTLA4* or anti-*PD1* drugs alone and no ICIs. Among them, the ordinate IPS represents the treatment state (higher IPS represents more benefits); neg implies that no blocker was used, and pos represents the use of a blocker. (B) Patients with high API show greater sensitivity to chemotherapeutic agents (lower $IC_{50}$ values), namely paclitaxel and cisplatin. API: autophagy-related prognostic index; IC: inhibitory concentration.

correspond to a concomitant 50% death rate. Due to the small number of patients, this cohort might be prone to a large bias. We speculate that with the increase in the number of patients, an intersection between the two curves may not be present and this needs to be verified. The API showed satisfactory accuracy in prognostic prediction for patients with CESC and can be employed independently in the clinic. The nomogram was a readable chart constructed based on hub AEG expression and clinicopathological variables. It could offer more accurate predictions for CESC prognosis.

In order to understand the molecular nature of the API, we assessed mutations in patients with high versus low API. Previous studies have reported frequent mutations in genes, including *SH3KBP1 binding protein 1* (*SHKBP1*), *caspase 8* (*CASP8*), *major histocompatibility complex, class I, A* (*HLA-A*), *phosphatidylinositol-4,5-bisphosphate 3-kinase catalytic subunit alpha* (*PIK3CA*), *tumor protein p53* (*TP53*), and *titin* (*TTN*) in patients with CESC [33, 34], which are partially consistent with our results. In this study, high mutation rates were found in *TTN*, *PIK3CA*, *KMT2C*, *MUC4*, and *MUC16*, which were mostly of the missense type. Mutations in *MUC16* showed the most genetic variations in patients with high versus low API. Upregulation of *MUC16* promotes CESC progression via the Janus kinase 2/signal transducer and activator of transcription 3 (JAK2/STAT3) pathway [35] and is associated with a lower survival rate [36]. However, *MUC16* mutations are significantly associated with a better prognosis in gastric cancer [37]. Therefore, tumor proliferation may be promoted in patients with low API through the abnormally activated JAK/STAT pathway, consistent with our results of survival analysis.

In the current study, the tumor-infiltrating immune cell landscape was profiled to examine the immune characteristics of API. High API correlated with increased infiltration of CD8$^+$ T cells and Tregs, and inhibition of infiltration of activated NK cells and activated DCs. The predominant CD8$^+$ T cell responses can boost an adequate immune response [38] and are the preferred mechanisms underlying successful immunotherapeutic strategies. However, Tregs often defend against autoimmunity, thus inhibiting antitumor immune responses and facilitating cancer progression [39]. NK cell infiltration is significantly associated with prolonged survival of cancer patients and the success of immunotherapy [40, 41]. In light of these intricate relationships among immune cells, it is still too early to conclude the efficacy of API in predicting tumor occurrence or development by evaluating the immune cell landscape of individual patients and requires further validation.

Subsequently, the relationships between API and known biomarkers of immunotherapeutic response prediction, such as immune checkpoints *PD-L1* and *PD-1*, were evaluated. Accumulating evidence has ascertained the favorable performance of immune checkpoints in assessing and monitoring immunotherapeutic outcomes in cancer patients [42, 43]. In this study, API could identify aberrantly expressed immune checkpoint genes and predict patients' responses to common ICIs and chemotherapeutic agents. Six immune checkpoint genes, including *PD-1*, *PD-L1*, *CTLA4*, *TIM-3*, *TIGIT* and *VISTA*, were upregulated in tumor tissues of patients with high

API. Patients with high API may benefit more from ICI treatment. Our results of immunotherapeutic response prediction also proved that patients with high API are more sensitive to *PD1* and *CTLA4* inhibitors than those with low API. API is a prognostic marker based on two autophagy genes and can reflect the autophagy state of the tumor. Autophagy deficiency in tumors may result in genomic instability and anticancer drug resistance. Autophagy pathways are crucial for TME regulation including those of immune responses [44], which may underlie the key to resistance against immunotherapy. Interestingly, the above results are consistent with those of chemotherapy prediction, whereby patients with low API were less sensitive to cisplatin and paclitaxel. This may be due to autophagy deficiency resulting in genomic instability and the development of anti-cancer drug resistance [45]. Therefore, the API based on three culprit AEGs responsible for CESC progression could successfully distinguish low-risk patients (with high API) from high-risk patients and is worthy of application to risk stratification and development of personalized treatment for CESC patients.

## 5. Conclusions

In conclusion, low levels of ARG expression (*BCL2*, *ATG4D* and *TP73*) were the Achilles' heels for CESC. API could accurately predict the prognosis and efficacy of immunotherapy and chemotherapy in patients with CESC. However, our conclusions require further experimental validation in future studies.

### AVAILABILITY OF DATA AND MATERIALS

The data presented in this study are available on reasonable request from the corresponding author.

### AUTHOR CONTRIBUTIONS

LZ—designed the research study. YG—performed the research. HY and YW—analyzed the data. LZ and YG—wrote the manuscript. All authors read and approved the final manuscript.

### ETHICS APPROVAL AND CONSENT TO PARTICIPATE

Due to the retrospective nature of the study, ethical approval was abandoned. The data used in this study were downloaded from the TCGA database (https://gdc.cancer.gov/).

### ACKNOWLEDGMENT

### FUNDING

## CONFLICT OF INTEREST

The authors declare no conflict of interest.

## SUPPLEMENTARY MATERIAL

Supplementary material associated with this article can be found, in the online version, at https://oss.ejgo.net/files/article/1779747092062715904/attachment/Supplementary%20material.zip.

## REFERENCES

[1] Bray F, Ferlay J, Soerjomataram I, Siegel RL, Torre LA, Jemal A. Global cancer statistics 2018: GLOBOCAN estimates of incidence and mortality worldwide for 36 cancers in 185 countries. CA: A Cancer Journal for Clinicians. 2018; 68: 394–424.

[2] Sharma S, Deep A, Sharma AK. Current treatment for cervical cancer: an update. Anti-Cancer Agents in Medicinal Chemistry. 2020; 20: 1768–1779.

[3] Eskander RN, Tewari KS. Chemotherapy in the treatment of metastatic, persistent, and recurrent cervical cancer. Current Opinion in Obstetrics & Gynecology. 2014; 26: 314–321.

[4] Rose PG, Bundy BN, Watkins EB, Thigpen JT, Deppe G, Maiman MA, et al. Concurrent cisplatin-based radiotherapy and chemotherapy for locally advanced cervical cancer. The New England Journal of Medicine. 1999; 340: 1144–1153.

[5] Bellmunt J, de Wit R, Vaughn DJ, Fradet Y, Lee JL, Fong L, et al. Pembrolizumab as second-line therapy for advanced urothelial carcinoma. The New England Journal of Medicine. 2017; 376: 1015–1026.

[6] Yang S, Zhang Z, Wang Q. Emerging therapies for small cell lung cancer. Journal of Hematology & Oncology. 2019; 12: 47.

[7] Chung HC, Ros W, Delord JP, Perets R, Italiano A, Shapira-Frommer R, et al. Efficacy and safety of pembrolizumab in previously treated advanced cervical cancer: results from the phase II KEYNOTE-158 study. Journal of Clinical Oncology. 2019; 37: 1470–1478.

[8] Naumann RW, Hollebecque A, Meyer T, Devlin M, Oaknin A, Kerger J, et al. Safety and efficacy of nivolumab monotherapy in recurrent or metastatic cervical, vaginal, or vulvar carcinoma: results from the phase I/II Checkmate 358 trial. Journal of Clinical Oncology. 2019; 37: 2825–2834.

[9] Ventriglia J, Paciolla I, Pisano C, Cecere SC, Di Napoli M, Tambaro R, et al. Immunotherapy in ovarian, endometrial and cervical cancer: State of the art and future perspectives. Cancer Treatment Reviews. 2017; 59: 109–116.

[10] Otter SJ, Chatterjee J, Stewart AJ, Michael A. The role of biomarkers for the prediction of response to checkpoint immunotherapy and the rationale for the use of checkpoint immunotherapy in cervical cancer. Clinical Oncology. 2019; 31: 834–843.

[11] Kondo Y, Kanzawa T, Sawaya R, Kondo S. The role of autophagy in cancer development and response to therapy. Nature Reviews Cancer. 2005; 5: 726–734.

[12] Li X, He S, Ma B. Autophagy and autophagy-related proteins in cancer. Molecular Cancer. 2020; 19: 12.

[13] Xia H, Green DR, Zou W. Autophagy in tumour immunity and therapy. Nature Reviews Cancer. 2021; 21: 281–297.

[14] Gerada C, Ryan KM. Autophagy, the innate immune response and cancer. Molecular Oncology. 2020; 14: 1913–1929.

[15] White E, Mehnert JM, Chan CS. Autophagy, Metabolism, and Cancer. Clinical Cancer Research. 2015; 21: 5037–5046.

[16] Newman AM, Liu CL, Green MR, Gentles AJ, Feng W, Xu Y, et al. Robust enumeration of cell subsets from tissue expression profiles. Nature Methods. 2015; 12: 453–457.

[17] Frenel JS, Le Tourneau C, O'Neil B, Ott PA, Piha-Paul SA, Gomez-Roca C, et al. Safety and efficacy of pembrolizumab in advanced, programmed death ligand 1-positive cervical cancer: results from the phase Ib KEYNOTE-028 trial. Journal of Clinical Oncology. 2017; 35: 4035–4041.

[18] Mayadev JS, Enserro D, Lin YG, Da Silva DM, Lankes HA, Aghajanian C, et al. Sequential ipilimumab after chemoradiotherapy in curative-intent treatment of patients with node-positive cervical cancer. JAMA Oncology. 2020; 6: 92–99.

[19] Colombo N, Dubot C, Lorusso D, Caceres MV, Hasegawa K, Shapira-Frommer R, et al. Pembrolizumab for persistent, recurrent, or metastatic cervical cancer. The New England Journal of Medicine. 2021; 385: 1856–1867.

[20] Duska LR, Scalici JM, Temkin SM, Schwarz JK, Crane EK, Moxley KM, et al. Results of an early safety analysis of a study of the combination of pembrolizumab and pelvic chemoradiation in locally advanced cervical cancer. Cancer. 2020; 126: 4948–4956.

[21] Mizushima N, Komatsu M. Autophagy: renovation of cells and tissues. Cell. 2011; 147: 728–741.

[22] Harris J. Autophagy and cytokines. Cytokine. 2011; 56: 140–144.

[23] Yamamoto K, Venida A, Yano J, Biancur DE, Kakiuchi M, Gupta S, et al. Autophagy promotes immune evasion of pancreatic cancer by degrading MHC-I. Nature. 2020; 581: 100–105.

[24] Robainas M, Otano R, Bueno S, Ait-Oudhia S. Understanding the role of PD-L1/PD1 pathway blockade and autophagy in cancer therapy. OncoTargets and Therapy. 2017; 10: 1803–1807.

[25] Zhong Z, Sanchez-Lopez E, Karin M. Autophagy, inflammation, and immunity: a troika governing cancer and its treatment. Cell. 2016; 166: 288–298.

[26] Bortnik S, Gorski SM. Clinical applications of autophagy proteins in cancer: from potential targets to biomarkers. International Journal of Molecular Sciences. 2017; 18: 1496.

[27] Ma M, Xie W, Li X. Identification of autophagy-related genes in the progression from non-alcoholic fatty liver to non-alcoholic steatohepatitis. International Journal of General Medicine. 2021; 14: 3163–3176.

[28] Hardwick JM, Soane L. Multiple functions of BCL-2 family proteins. Cold Spring Harbor Perspectives in Biology. 2013; 5: a008722.

[29] Martínez-Arribas F, Alvarez T, Del Val G, Martín-Garabato E, Núñez-Villar MJ, Lucas R, et al. Bcl-2 expression in breast cancer: a comparative study at the mRNA and protein level. Anticancer Research. 2007; 27: 219–222.

[30] Yao Q, Chen J, Lv Y, Wang T, Zhang J, Fan J, et al. The significance of expression of autophagy-related gene Beclin, Bcl-2, and Bax in breast cancer tissues. Tumour Biology. 2011; 32: 1163–1171.

[31] Logotheti S, Richter C, Murr N, Spitschak A, Marquardt S, Pützer BM. Mechanisms of functional pleiotropy of p73 in cancer and beyond. Frontiers in Cell and Developmental Biology. 2021; 9: 737735.

[32] Ye H, Guo X. TP73 is a credible biomarker for predicting clinical progression and prognosis in cervical cancer patients. Bioscience Reports. 2019; 39: BSR20190095.

[33] Zhang L, Jiang Y, Lu X, Zhao H, Chen C, Wang Y, et al. Genomic characterization of cervical cancer based on human papillomavirus status. Gynecologic Oncology. 2019; 152: 629–637.

[34] Burki TK. Novel mutations in cervical cancer. The Lancet. Oncology. 2017; 18: e137.

[35] Shen H, Guo M, Wang L, Cui X. MUC16 facilitates cervical cancer progression via JAK2/STAT3 phosphorylation-mediated cyclooxygenase-2 expression. Genes & Genomics. 2020; 42: 127–133.

[36] Togami S, Nomoto M, Higashi M, Goto M, Yonezawa S, Tsuji T, et al. Expression of mucin antigens (MUC1 and MUC16) as a prognostic factor for mucinous adenocarcinoma of the uterine cervix. The Journal of Obstetrics and Gynaecology Research. 2010; 36: 588–597.

[37] Li X, Pasche B, Zhang W, Chen K. Association of MUC16 mutation with tumor mutation load and outcomes in patients with gastric cancer. JAMA Oncology. 2018; 4: 1691–1698.

[38] Farhood B, Najafi M, Mortezaee K. CD8(+) cytotoxic T lymphocytes in cancer immunotherapy: a review. Journal of Cellular Physiology. 2019; 234: 8509–8521.

[39] Knochelmann HM, Dwyer CJ, Bailey SR, Amaya SM, Elston DM, Mazza-McCrann JM, et al. When worlds collide: Th17 and Treg cells in cancer and autoimmunity. Cellular & Molecular Immunology. 2018; 15: 458–469.

[40] Bigley AB, Simpson RJ. NK cells and exercise: implications for cancer

immunotherapy and survivorship. Discovery Medicine. 2015; 19: 433–445.

[41] Shimasaki N, Jain A, Campana D. NK cells for cancer immunotherapy. Nature Reviews Drug Discovery. 2020; 19: 200–218.

[42] Sun C, Mezzadra R, Schumacher TN. Regulation and function of the PD-L1 checkpoint. Immunity. 2018; 48: 434–452.

[43] Gibney GT, Weiner LM, Atkins MB. Predictive biomarkers for checkpoint inhibitor-based immunotherapy. The Lancet. Oncology. 2016; 17: e542–e551.

[44] Yamazaki T, Bravo-San Pedro JM, Galluzzi L, Kroemer G, Pietrocola F. Autophagy in the cancer-immunity dialogue. Advanced Drug Delivery Reviews. 2021; 169: 40–50.

[45] Yousefi S, Simon HU. Autophagy in cancer and chemotherapy. Results and Problems in cell Differentiation. 2009; 49: 183–190.